

Molecular diffusion and nuclear-magnetic-resonance relaxation of water in unsaturated porous silica glass

Franco D'Orazio, Sankar Bhattacharja, and William P. Halperin
Department of Physics and Astronomy, Northwestern University, Evanston, Illinois 60208

Kiyohisa Eguchi
Government Industrial Research Institute, Osaka, Ikeda, Japan

Takao Mizusaki
Department of Physics, Kyoto University, Kyoto, Japan
(Received 9 July 1990)

Measurements have been performed of the nuclear-magnetic-resonance longitudinal and transverse relaxation and the self-diffusion coefficient of deionized water confined in the porous space of a silica glass. The average pore diameter of the glass is 3.5 nm, and the experiments were conducted with different degrees of fluid filling. All three physical quantities were found to be linearly dependent on filling provided this was in excess of the amount of water corresponding to one monolayer, in agreement with theoretical predictions based on geometrical considerations. However, a deviation is observed below one monolayer, which is interpreted as a modification of the liquid-solid interface interaction, which causes the water molecules to become less mobile.

I. INTRODUCTION

Considerable effort has been devoted to the characterization of various porous materials, to study the physical properties of fluids inserted in their porous structure, and to determine the relationship between these two aspects.¹ This investigation has both fundamental and technological interests. Sample formation, catalytic reactions, chromatography, hydrocarbon recovery, and superfluidity in restricted geometry are a few examples. Nuclear-magnetic-resonance (NMR) relaxation and diffusion measurements have played an important role contributing extensively to the understanding of porous structures and fluid transport properties in random geometries. In particular, relaxation measurements on liquids filling the pore space probe the internal local surface-to-volume ratio and, therefore, determine pore-size distributions.^{2,3} Pulsed magnetic field gradient (PFG) NMR self-diffusion measurements provide direct information about the local mean-square displacement of molecules over a wide range of time scales, revealing the presence of inhomogeneity, self-similarity, anisotropy of samples, and measuring directly the geometrical restriction to transport due to the pore structure.⁴

The dependence of the experimentally observed quantities on the degree of fluid impregnation in the porous materials has also been addressed, both theoretically⁵ and experimentally.^{2,4,6,7} This procedure examines more extensively the liquid-solid interface interaction, which is responsible for the enhanced relaxation rate observed in NMR experiments. It is also essential to the interpretation of the mechanism for diffusion, since it provides information about connectivity of the porous space and about the possible influence of surface transport to the

observed phenomena.

In this paper we report results of NMR relaxation and diffusion experiments on water filling a well-characterized porous silica glass (0.35 in porosity, 3.5 nm in pore diameter). We describe the dependence of the relaxation times and self-diffusion coefficient on the amount of water imbibed into the sample. The range of water content covers that from saturated conditions down to submonolayer surface coverage of the wetting liquid. At exactly one monolayer a change in the trend of the measured parameters as a function of water content is observed. We attribute this to a crossover from bulk to surface transport behavior of the water molecules.

II. THEORY OF NMR IN PORUS MATERIALS

A. Relaxation

The suitability of NMR relaxation experiments in studying porous media is due to an observed enhanced relaxation rate of liquids when inserted in the open space of the material. This feature is attributed to interactions involving the probing molecules at the liquid-solid interface. Although speculations about the origin of this interaction have been made, no conclusion has been reached and it is possible that different contributions may be more or less effective, depending on the sample composition and the nature of the filling liquid. Typically, effects such as the presence of paramagnetic impurities and physisorption are considered to be key aspects of the phenomenon. In many applications knowledge of the specific nature of the enhanced relaxation is not required, provided that some assumptions are made which allow the definition of phenomenological parameters describing the character of the interactions. The characterization of

porous materials via relaxation techniques is a case in point. If a short-range surface interaction is present and there is a fast exchange of molecules between the surface region and the remaining part of the liquid in the sample during the time of the experiment, then the induced nuclear magnetization $M(t)$, normalized to its initial value $M(0)$, is expected to relax exponentially in time:

$$A(t) = \frac{M(t)}{M(0)} = \exp\left[-\frac{t}{T'}\right], \quad (1)$$

with a relaxation rate given by the weighted average between the surface and the bulk rates:

$$\frac{1}{T'} = \left[1 - \frac{\lambda s}{v}\right] \frac{1}{T_b} + \frac{\lambda s}{v} \frac{1}{T_s}, \quad (2)$$

where T_b and T_s refer to bulk and surface relaxation times, respectively; s and v represent the local surface area and pore volume, respectively; and λ is a length representing the extension of the surface interaction responsible for the enhanced relaxation. Equations (1) and (2) are valid for both longitudinal (T_1) and transverse (T_2) relaxation decays, and they define the local contribution to the NMR signal. The term "local" refers to the confined region visited by each molecule during the NMR excitation-detection time interval. The size of this region depends on the diffusion coefficient of the liquid in the porous structure, and it is typically a few micrometers in the case of water. It must be larger than the characteristic pore size in order to ensure that the condition for fast molecular exchange holds as mentioned above. In Eq. (2) the parameter λ is expected to be of the order of one intermolecular distance since it represents the nuclear dipole-dipole interaction range. This expectation is confirmed in the experiments reported here. Consequently, the volume of liquid which experiences this interaction at each instant is approximately proportional to λs . A correction is required for geometries characterized by pore sizes comparable with λ .⁸

A more convenient way to express Eq. (2) is

$$T = \frac{v}{s\rho}, \quad (3)$$

where the relevant relaxation time T is related to the measured T' by

$$\frac{1}{T} \equiv \frac{1}{T'} - \frac{1}{T_b}, \quad (4)$$

and the surface relaxation strength ρ is given by

$$\rho \equiv \lambda \left[\frac{1}{T_s} - \frac{1}{T_b} \right], \quad (5)$$

which represents a phenomenological physical constant characteristic of the liquid-solid system. Usually, T and T' do not differ appreciably, since $T_s \ll T_b$. In general, the local relaxation times may vary throughout the sample, due to different local surface-to-volume ratios. In that case, multiexponential recovery of the nuclear magnetization is observed:

$$A(t) = \int_0^\infty P(T') \exp\left[-\frac{t}{T'}\right] dT', \quad (6)$$

and an analysis may provide the distribution of relaxation times $P(T')$. In turn, this gives a pore-size distribution where size is related to the surface-to-volume ratio by an assumed pore shape.^{2,3}

When a nonexponential decay of the nuclear magnetization is observed, due either to a distribution of local surface-to-volume ratios or to slower molecular exchange, then a more global relation than Eq. (3) still applies:

$$T_{av} = \frac{V}{S\rho}, \quad (7)$$

where T_{av} is the inverse of the average relaxation rate of the liquid in the entire sample, S is the total area of the liquid-solid interface, and V the total volume occupied by the liquid. The parameter ρ is considered to be constant throughout the sample, as a consequence of the supposed homogeneity of the properties of the surface. T_{av} can be extracted from the experimental relaxation recovery and can be shown to be given by^{2,3}

$$\frac{1}{T_{av}} = \left[-\frac{d}{dt} \ln A(t) \right]_{t=0}. \quad (8)$$

Clearly, for a single exponential decay, Eqs. (3) and (7) coincide.

Equation (7) provides a simple relation between the relaxation time and the surface-to-volume ratio. If the surface interaction length were comparable with the characteristic pore size, then the dependence of the relaxation time on the surface area would deviate from that shown in Eq. (7), but this would not affect its proportionality with the volume. The expected linearity between relaxation times and volume of liquid, even for samples with small pore sizes or rough surfaces, has an application in coverage studies, in which the amount of the probing liquid in the sample is progressively varied and the corresponding relaxation time measured. If the liquid is a wetting fluid, a change in filling does not affect the value of S . Then the observed relaxation time is expected to be linear with liquid content.

Equation (3) or (7) is valid only at filling corresponding to multilayer surface coverage, that is, for $\lambda S \leq V$. When one monolayer is approached, all the liquid molecules are interacting with the solid interface and the measured relaxation time T' coincides with the surface value T_s . Below one monolayer, T' is identically equal to T_s , but the latter value may evolve as the monolayer correlation times change with concentration of molecules in the adsorbed monolayer.

B. Self-diffusion

No rigorous theory about self-diffusion of fluid molecules in porous media has been developed so far. This transport property has been commonly related to dc conductivity of saline solutions through the Einstein equation

$$\frac{\mu_{\text{ion}}}{D_{\text{ion}}} = \frac{q_{\text{ion}}}{k_B T}, \quad (9)$$

which leads to

$$\frac{\sigma}{\sigma_0} = \frac{D}{D^0} \frac{V}{V_T}. \quad (10)$$

In the two equations above, μ_{ion} , D_{ion} , and q_{ion} are, respectively, the mobility, the self-diffusion coefficient, and the electrical charge of any ionic species present in the solution; k_B is the Boltzmann constant, T the temperature, σ and D , respectively, the conductivity of the solution and self-diffusion of molecules in the liquid within the porous geometry, σ_0 and D^0 the corresponding bulk values, and V_T the total volume of the sample. Equation (10) is valid when the ratio between the transport parameters of the fluids inside the porous medium and those of the bulk fluids are the same for all ions or molecules considered. This is true when geometrical factors alone affect the transport properties, that is, when the molecular and ionic interactions associated with the liquid-solid interface are not appreciable.

Both transport properties are found to be hindered with respect to their corresponding bulk properties, due to the increased tortuosity of the transport path. There is a widely accepted phenomenological relationship between conductivity and porosity known as Archie's law:⁹

$$\frac{\sigma}{\sigma_0} = \phi^{p'} \left[\frac{V}{V_0} \right]^p. \quad (11)$$

The porosity ϕ is defined as the ratio between the volume V_0 accessible to an external fluid and the total sample volume V_T ; the exponents p' and p , which are empirical, have no rigorous theoretical explanation and usually range between 1.5 and 2, depending on the set of samples under examination. We emphasize that the topology of the liquid contained in a completely filled pore space may be different from that of the liquid that only partly fills this space. This is the reason we formally allow a difference between the exponents p and p' . The phenomenological result of Eq. (11) and the theoretical relation given in Eq. (10) provide the following expression for the self-diffusion coefficient:

$$\frac{D}{D^0} = \phi^{p'-1} \left[\frac{V}{V_0} \right]^{p-1}. \quad (12)$$

This result takes into account only the geometrical consequences implied by the drying process, and therefore a deviation from the dependence predicted by Eq. (12) might be expected for water content approaching one monolayer if one assumes different transport properties for adsorbed molecules.

Recently, we have reported an anomalous dependence of the diffusion coefficient of liquid water as a function of filling observed for a set of porous silica glasses characterized by high porosity ($\phi=0.85$) and relatively large pore size (of the order of 100 nm).⁴ In that case, the observed increase of diffusion with decreasing water content was attributed to the indirect contribution of vapor to the

molecular transport in the liquid. To our knowledge, this is the only reported observation of such behavior. The mathematical model developed for that case satisfactorily fitted the experimental data. However, some questions remain about the generality of this result, since the details of the contribution of the vapor phase are not well understood.⁷ In the following sections we will also try to address this problem and determine when the vapor phase is expected to influence molecular transport.

III. SAMPLE PREPARATION AND CHARACTERIZATION

The sample used in this experiment is a porous glass prepared by the method of Tanaka *et al.*:¹⁰ the pore structure is generated by acid leaching the borate phase of a phase-separated soda borosilicate glass. This procedure can generate samples with pore structure having two characteristic sizes.² The heat-treatment conditions determine the coarse pore size; the presence of fine pores is due to colloidal silica particles precipitated from the acid soluble borate phase in the coarser porous skeleton structure after acid leaching. With low acid-to-glass ratios and short leaching times, only the borate phase is dissolved; the colloidal particles are not removed and they define a homogeneous fine-pore structure. This is the type of sample we have used. Additional details about the preparation of these glasses are described in Ref. 10.

The original sample was a rod of 0.4 cm in diameter. For the purpose of our investigation, it was cut into a number of cylinders about 1 cm long, using a water-lubricated diamond saw. After cutting, the sample was washed in de-ionized water and dried by heating in vacuum at 110°C for several hours. Nitrogen sorption measurements were performed after removing the sample from the furnace. The dry weight of the sample was measured on a microbalance after further evacuation. Finally, the sample was reimpregnated by placing it in a beaker filled with de-ionized water. The fluid imbibed spontaneously into the pores by capillary wetting. After removal from the fluid, the external surface was wiped using an absorbant tissue. The sample was then promptly reweighted; the difference with respect to the dry weight was used to calculate the open pore volume V_0 . To obtain measurements under saturated conditions, the sample was then immediately placed at the bottom of an NMR tube and sealed after filling the rest of the tube with a Teflon rod in order to minimize evaporation. For measurements under unsaturated conditions, the sample was subsequently exposed to air and allowed to dry partially on the microbalance before reinserting and sealing it in the NMR tube. For lower filling, when the water did not evaporate spontaneously, the sample was dried more extensively in an oven and then placed on the microbalance so that it could gain water from moisture in the air. In all cases the amplitude of the NMR spin-echo signal extrapolated to zero time was found to be proportional to the amount of water measured from the recorded weight. This result effectively proves that evaporation from the sample did not take place after sealing the NMR tube to an accuracy of roughly 2%.

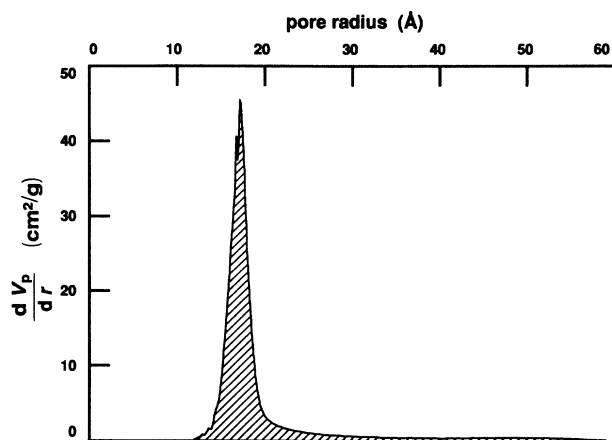


FIG. 1. Pore-volume distribution as a function of pore size for the glass sample as obtained from the analysis of the nitrogen desorption isotherm at liquid-nitrogen temperature.

Mercury porosimetry revealed a negligible intruded volume of the nonwetting liquid into the sample, proving that no substantial portion of the porous structure was described by geometrical sizes larger than a few nanometers. Therefore, the porous material was characterized by nitrogen sorption techniques using an Omnisorp 360, Omicron Technology Co., apparatus. The measured surface area per unit weight of glass, deduced from Brunauer-Emmett-Teller (BET) analysis of the nitrogen adsorption isotherm at liquid-nitrogen temperature, was $210 \text{ m}^2/\text{g}$, with an accuracy of 10%. The total pore volume calculated from nitrogen desorption was $0.25 \text{ cm}^3/\text{g}$. A slightly smaller value was obtained by measuring the weight of water spontaneously imbibing into the glass, as described above, and is believed to be more accurate. This value is $0.22 \text{ cm}^3/\text{g}$, and it is consistent with that derived from the geometrical dimensions of the sample, assuming that the bulk mass density of the glass is $2.1 \text{ g}/\text{cm}^3$. Therefore, in the discussion later, the value $V_0 = 0.22 \text{ cm}^3/\text{g}$ will be used. This corresponds to a porosity $\phi = 0.35$. The pore size distribution from the desorption curve is shown in Fig. 1 and consists of a narrow peak centered at a pore diameter $d = 3.5 \text{ nm}$.

IV. EXPERIMENTAL TECHNIQUES

Pulsed NMR transverse (T_2) and longitudinal (T_1) relaxation measurements were performed on the sample at room temperature. For T_2 measurements the Carr-Purcell-Meiboom-Gill (CPMG) pulse sequence¹¹ $\pi/2-(\tau-\pi-\tau-\text{echo})_N$ was used, in order to eliminate signal attenuation due to diffusion in the background inhomogeneous magnetic field. In this sequence the experimental time variable is represented by the quantity $t = 2N\tau$; the value of τ chosen depended on the particular filling condition, and at low coverage was as small as $50 \mu\text{s}$. The echo amplitude following each of the π pulses was recorded after averaging the signal for many subsequent identical pulse sequences separated by an appropriate waiting time. T_1

measurements were performed using a $(\pi-t-\pi/2-\tau'-\pi-\tau'-\text{echo})$ inversion recovery sequence. The echo amplitude was detected as a function of the time variable t , using a similar signal averaging procedure. The parameter τ' was kept constant, at a value of a few hundred microseconds.

Self-diffusion measurements were performed at room temperature using the NMR PFG technique. The PFG was superimposed on a stimulated echo-pulse sequence, as described by Tanner.¹² This technique is more appropriate when the characteristic longitudinal relaxation times are much longer than the transverse relaxation times and when relatively slow molecular diffusion occurs. The time interval Δ between the two identical magnetic gradient pulses was varied keeping their time duration δ and intensity g constant for each water filling. In this way the ratio R between the echo amplitude with and without the presence of the PFG can be expressed more generally as

$$R = \exp \left[-(\gamma g \delta)^2 \frac{\langle r(t)^2 \rangle}{6} \right], \quad (13)$$

where γ is the gyromagnetic ratio and $\langle r(t)^2 \rangle$ is the mean-square displacement of a water molecule during the time $t \equiv \Delta - \delta/3$.

With this technique direct information about the evolution of the mean-square displacement of water molecules with time is obtained. In particular, it can be determined if classical diffusion occurs during the range of time intervals explored by the measurements. If this is the case, the mean-square displacement is linearly time dependent, and in three dimensions the relation $\langle r(t)^2 \rangle = 6Dt$ holds, which defines the proportionality constant D referred to as the self-diffusion coefficient. Equation (13) becomes

$$R = \exp[-D(\gamma g \delta)^2 t], \quad (14)$$

and the experimental verification of this time dependence constitutes evidence of classical molecular diffusion.

V. RESULTS AND DISCUSSION

Longitudinal and transverse relaxation measurements at different water contents were performed at 27 and 11 MHz. Some longitudinal relaxation measurements were performed at 400 MHz. The nuclear magnetization decays were exponential in time at high coverage, but they exhibited a small deviation as one monolayer was approached. However, this deviation was so small that a quantitative analysis in order to distinguish the multicomponent character of the relaxation was not possible. For this reason, the physically meaningful quantity which will be discussed is the average relaxation time, defined in Eq. (8), which, from now on, will be simply referred to as T_1 or T_2 . According to Eqs. (7) or (3), the relaxation rate multiplied by the volume of water should be a constant for a wetting fluid. This is verified by plotting, as a function of the fraction V/V_0 of the total pore volume occupied by water, the relaxation rate times the fraction V/V_0 itself. Figures 2 and 3 show the results of the lon-

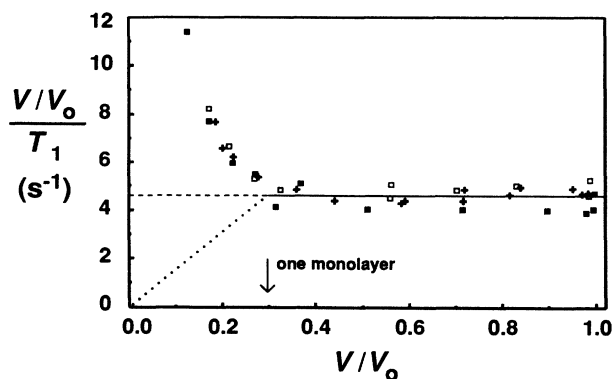


FIG. 2. Longitudinal relaxation rate of the proton nuclear magnetization multiplied by V/V_0 as a function of V/V_0 . The fraction V/V_0 represents the ratio between the volume V of water and the total open-pore volume V_0 of the glass sample. Different symbols refer to distinct sets of data: (■), (□), 27-MHz resonance frequency, (+) 11 MHz. The first data set (■) was collected a few months before the others. The horizontal line represents the best fit of the data above one monolayer to Eq. (7). The dotted line is the expected behavior if there is no change in the interaction responsible for relaxation during drying in the submonolayer region.

gitudinal and transverse relaxation experiments, respectively, for three different sets of data corresponding to different cycles of drying and reimbibing with water.

The salient features of these plots are the large difference between T_1 and T_2 values at all water contents, the constancy of both plots above $V/V_0=0.3$, and a different trend below that value. This is more marked in the plot of the longitudinal relaxation, but it is apparent also for the transverse relaxation. The value $V/V_0=0.30$ indicates a geometrical characteristic of this liquid-solid system. In fact, it corresponds to one adsorbed monolayer of water, as obtained from the relation $\lambda S/V_0$, using the surface-area value reported in Sec. III and taking the thickness of a water layer to be $\lambda=0.3$ nm. In this

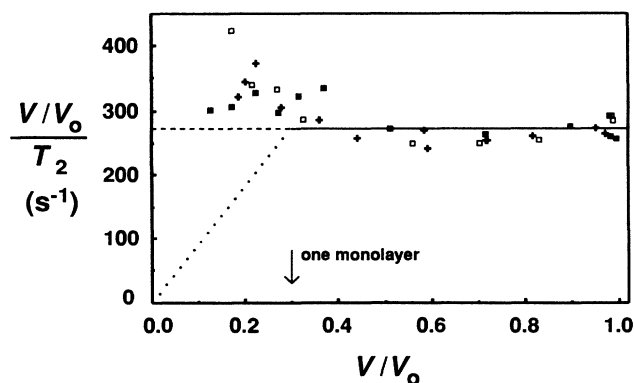


FIG. 3. Transverse relaxation rate of the proton nuclear magnetization multiplied by V/V_0 as a function of V/V_0 . The symbols have a similar meaning to those used in Fig. 2.

calculation the area covered by one monolayer of nitrogen during the adsorption experiment and the area covered by the first monolayer of water are assumed to be the same. To a first approximation a correction to the volume λS of a monolayer to account for the curvature of the surface is not needed since this error is compensated by a similar error in the value of the surface area S calculated from the volume of nitrogen adsorbed.

The linearity of the relaxation times as a function of the volume of water contained in the sample above one monolayer is similar to our earlier reports^{2,6} on other glass samples. This result, combined with the observation that the relaxation decay is always exponential in this region of water filling, allows three important conclusions: that the sample dries uniformly, that it wets the solid surface, and that the conditions for fast molecular exchange are satisfied. Moreover, the surface interaction parameter ρ appears to be a well-defined quantity at least for coverages down to one monolayer, indicating that from Eq. (5) the interaction length λ corresponds to one molecular distance. In other words, all water molecules not included in the first adsorbed layer and in the absence of exchange with the surface layer would have a relatively long relaxation time, presumably the same as for bulk water. Also, this result implies that the physical interactions experienced by the first water layer and responsible for the enhanced relaxation are not altered when all the other molecules are removed. Therefore, the surface relaxation is not due to interactions between molecules in different (i.e., first and second) layers. From the fitting of the linear region shown in Figs. 2 and 3, and using Eq. (7), we obtain $\rho_1=4.6$ nm/s and $\rho_2=270$ nm/s. These values are calculated from an average over the three data sets whose relative deviation is a few percent. According to Eq. (5), with $T_b \approx 3$ s for both longitudinal and transverse relaxation of bulk water, these correspond to surface relaxation times $T_{1s}=64$ ms and $T_{2s}=1.10$ ms. Both the large difference between the two relaxation rates and their submonolayer dependence on filling reflect the details of the surface interaction. This is in contrast to the region above one monolayer discussed before which has a purely geometrical origin. Interpretations of the surface interaction will be addressed later and compared with the results of the submonolayer self-diffusion measurements. A systematic difference between one data set (indicated with solid squares) and the others in Fig. 2 is attributed to the fact that this one was obtained a few months before the others, and therefore, a small change in surface conditions may have occurred in the interim. Sensitivity to chemically modified surface conditions has been noted by us earlier.²

PFG measurements were obtained for different V/V_0 ratios, varying the time interval Δ between magnetic gradient pulses from 3 to 100 ms. The resonance frequency in this case was 27 MHz. The time evolution duration δ of each gradient pulse was 0.5 ms and the intensity of the magnetic field gradient g was a few hundred G/cm, depending on the particular filling condition. In all cases the time dependence indicated in Eq. (14) was found, proving that classical diffusion was operative. The self-diffusion coefficient was calculated and is presented in

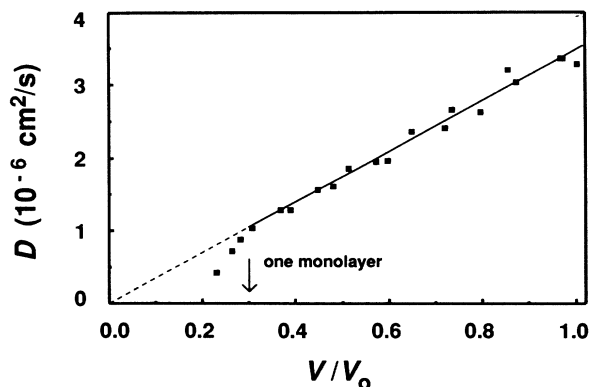


FIG. 4. Self-diffusion coefficient, obtained from NMR PFG experiments at room temperature and at 27-MHz resonance frequency, of water confined in the pore structure of the glass sample as a function of the ratio between the volume V of water and the total open-pore volume V_0 of the sample. The line represents the fitting using Eq. (12), Archie's law, with $p = 2$, for water filling above one monolayer.

Fig. 4 as a function of the water content V/V_0 .

The data at coverages above one monolayer may be fitted satisfactorily by a straight line. This is consistent with Eq. (12), where $p = 2$. An identical exponent was obtained recently from low-frequency electrical conductivity on a sol-gel silica glass sample with different pore-space characteristics ($\phi = 0.85$, $d = 240$ nm),⁷ suggesting that perhaps, for well-defined geometries with narrow pore-size distributions, this functionality is more than a phenomenological observation. Of course, the dependence on porosity cannot be checked since only one value of ϕ is available. However, assuming that the power law indicated in Eq. (12) is valid and using for the self-diffusion coefficient of bulk water at room temperature (25°C) $D^0 = 2.3 \times 10^{-5}$ cm²/s, we obtain $p' = 2.7$. The ratio D/D^0 for the saturated sample is almost twice the value measured by Fukuda *et al.*¹³ on a similar sample. However, it is similar to the value (0.17) derived from the ratio of helium gas diffusivity and the corresponding Knudsen value (which is the dominant gas diffusivity term in small pores) on Vycor glass,^{14,15} whose preparation and porous characteristics are essentially identical to those of the sample in the present investigation. It was suggested that this highly hindered transport is due to the peculiar structure of Vycor glass, which may be characterized by a collection of pores with a less interconnected structure than would be obtained by a random packing of particles.¹⁵ Another important factor hindering the transport process is the finite size of the diffusing molecules, not negligible with respect to the pore size.¹⁶

Interpretation of the relaxation and diffusion results in the interval corresponding to $V/V_0 < 0.3$, representing the submonolayer region, must take into account the possible evolution of the physical properties of the adsorbed water molecules upon drying. If no such modifications were present, then both relaxation times would remain constant during the entire interval and be equal to the

corresponding surface relaxation times according to the assumptions of Sec. II A. This would result in a linear plot represented in Figs. 2 and 3 as a dotted line through the origin. On the other hand, if only a part of the first monolayer molecules experienced the enhanced relaxation, for example, by assuming some inhomogeneity of the surface with strong binding sites, then the constancy of the plots in Figs. 2 and 3 would be maintained below one monolayer (following the dashed line) until the strongly bound molecules were also removed from the surface. From this point on, with further drying, a decrease of the curve would be observed. However, a different behavior is apparent in the experiments. Both relaxation rates *increase* with decreased filling below one monolayer. The longitudinal relaxation curve in Fig. 2 increases substantially above the value at high coverages; the transverse relaxation curve of Fig. 3 appears to increase before decreasing again at the lowest coverages. This result suggests that there is a change of the environment of the water molecules during drying affecting the relaxation process of the proton magnetization. A quantitative description of this phenomenon can be found invoking the theory of nuclear dipole-dipole interaction which is the dominant cause of relaxation for liquids.¹⁷ The large T_1/T_2 ratio and the small frequency dependence observed in our experiments are an indication that a single relaxation mechanism is not sufficient to describe the system.¹⁸ This conclusion was qualitatively discussed in our previous work on a series of leached borosilicate glasses prepared in a similar manner to the one described here.²

The simplest assumption is to consider that two distinct dynamical processes, represented by two correlation times, are present. The dominant cause of relaxation in water is the intramolecular magnetic dipolar proton-proton interaction. This process is regulated by the rotational degree of freedom of the molecule and the hypothesis that two processes are present may result from an anisotropy of such motion due to the solid surface, as originally suggested by Odajima, Sohma, and Watanabe for adsorbed water.¹⁹ One simple model is to assume that each molecule attached to the surface is relatively free to rotate around an axis perpendicular to the surface itself, with a characteristic correlation time τ_S , and that it is allowed occasionally to reorient around an axis parallel to the surface with characteristic time τ_L .^{18,20,21}

The relaxation rates for a molecule containing two nuclei of spin $\frac{1}{2}$ is given by²⁰

$$\frac{1}{T_i} = \frac{(3 \cos^2 \theta - 1)^2}{4T_i^{\text{iso}}(\omega, \tau_L)} + \frac{3 \sin^2 \theta \cos^2 \theta}{T_i^{\text{iso}}(\omega, \tau_\alpha)} + \frac{\frac{3}{4} \sin^4 \theta}{T_i^{\text{iso}}(\omega, \tau_\beta)}, \quad (15)$$

where θ is the angle between the preferential axis and the intramolecular proton-proton direction, and τ_α and τ_β are found from

$$\frac{1}{\tau_\alpha} = \frac{1}{\tau_L} + \frac{1}{\tau_S}, \quad \frac{1}{\tau_\beta} = \frac{1}{\tau_L} + \frac{4}{\tau_S}. \quad (16)$$

Equation (15) is obtained after averaging over all the possible orientations between the preferential rotational axis and the external magnetic field, which is appropriate for

a random medium with arbitrary orientation of the local solid-pore interface; the index $i = 1, 2$ refers to longitudinal and transverse relaxation time, respectively; the dependence of the relaxation rates on the correlation time τ for isotropic rotation and on the NMR resonance frequency $\omega/2\pi$ is given by

$$\frac{1}{T_1^{\text{iso}}} = \frac{3}{10} \frac{\gamma^4 \hbar^2}{r^6} \left[\frac{\tau}{1 + \omega^2 \tau^2} + \frac{4\tau}{1 + 4\omega^2 \tau^2} \right], \quad (17)$$

$$\frac{1}{T_2^{\text{iso}}} = \frac{3}{20} \frac{\gamma^4 \hbar^2}{r^6} \left[3\tau + \frac{5\tau}{1 + \omega^2 \tau^2} + \frac{2\tau}{1 + 4\omega^2 \tau^2} \right]. \quad (18)$$

In the two equations above, γ is the nuclear gyromagnetic ratio, \hbar the reduced Planck constant, and r the intramolecular proton-proton distance. Equation (15) holds for transverse relaxation ($i = 2$) only in the limit that T_2 is much larger than τ_L . If not, it must be replaced by the Kubo and Tomita relation,²² whose extreme limit for $\tau_L \gg T_2$ is

$$T_2 \approx \frac{2}{3} \frac{r^3}{\gamma^2 \hbar} \left[\frac{10}{\ln 2} \frac{1}{(3 \cos^2 \theta - 1)^2} \right]^{1/2}. \quad (19)$$

Equation (15), applied to longitudinal and transverse relaxation, constitutes a system of two equations from which the two correlation times can be calculated, once the angle θ is known. Because of our interpretation of the results shown in Figs. 2 and 3 above one monolayer, this entire region is characterized by the same constant surface relaxation time calculated from a best linear fit. Therefore, the two correlation times do not change in this interval and depend on coverage only below one monolayer. We will analyze our results treating the two most obvious configurations of the water molecules relative to the surface: (a) the intermolecular proton-proton direction is parallel to the surface ($\theta = 90^\circ$); (b) one of the O—H bonds is parallel to the surface and the other is contained in a plane perpendicular to it ($\theta = 52^\circ$).

Case (a) is consistent with water-surface bonding due to electric dipolar interaction of the molecules or for water hydrogen bonding with surface OH groups.¹⁸ In that situation Eq. (15) reduces to

$$\frac{1}{T_i} = \frac{1}{4} \frac{1}{T_i^{\text{iso}}(\omega, \tau_L)} + \frac{3}{4} \frac{1}{T_i^{\text{iso}}(\omega, \tau_\beta)}. \quad (15')$$

The values of the two correlation times τ_S and τ_L derived from the experimental relaxation times and from the expression above are reported in Fig. 5(a). Both correlation times are observed to increase with decreasing water filling, showing that the molecules become less mobile as the sample is dried. The observation that the two correlation times have the same trend suggests that they may have some common dynamical origin. This point will be discussed further in the context of the self-diffusion measurements. The values obtained for the two correlation times are in agreement with the estimate we have given previously for a set of samples of similar preparation.² However, a slightly multiexponential relaxation behavior

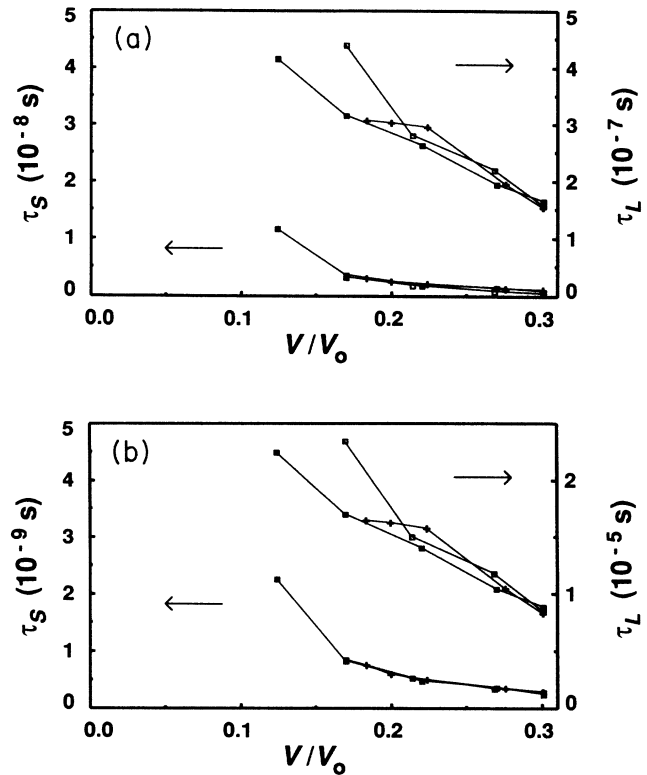


FIG. 5. Long (τ_L) and short (τ_S) correlation times as a function of the ratio between the volume V of water and the total open-pore volume V_0 of the glass sample, below one monolayer. The values are calculated interpreting the longitudinal and transverse relaxation experiments in terms of anisotropic motion of the water molecules adsorbed on the glass surface: (a) the intermolecular proton-proton direction is parallel to the surface; (b) one of the O—H bonds is parallel to the surface and the other is contained in a plane perpendicular to it. Different symbols refer to different data sets, as indicated in Fig. 2.

was observed in this region of coverage. Consequently, the present results may be taken to be semiquantitative, perhaps reflecting a certain degree of inhomogeneity present on the surface. The almost complete lack of frequency dependence of the measured relaxation times between 11 and 27 MHz at one monolayer is consistent with the values of the correlation times obtained from this calculation and with the finding that the Larmor period at each resonance frequency is intermediate between the two correlation times. In fact, in the extreme limit such that $\omega\tau_\beta \ll 1 \ll \omega\tau_L$, one would get, from Eq. (15'),

$$\frac{1}{T_1} \approx \frac{9}{8} \frac{\gamma^4 \hbar^2}{r^6} \tau_\beta, \quad (20)$$

$$\frac{1}{T_2} \approx \frac{9}{80} \frac{\gamma^4 \hbar^2}{r^6} \tau_L. \quad (21)$$

In this limit the longitudinal relaxation rate is determined by the short correlation time alone and the transverse relaxation rate by the long correlation time. However, in

our case the above inequality is only valid for a relatively restricted interval of frequencies, since τ_β and τ_L differ by only 2 or 3 orders of magnitude. Using the value of the two correlation times obtained for a monolayer, one would estimate, for example, that at 400 MHz the values of the relaxation times would be $T_1=560$ ms and $T_2=3.7$ ms for a saturated sample, showing an appreciable frequency dependence for the longitudinal relaxation time. This estimate is in agreement with an actual measurement performed using a narrow-band NMR spectrometer at 400 MHz; the value obtained in this case was $T_1=540\pm 20$ ms, which validates our interpretation of the relaxation mechanism as due to multiple correlation times.

For case (b), Eq. (15) becomes

$$\frac{1}{T_i} = \frac{0.0047}{T_i^{\text{iso}}(\omega, \tau_L)} + \frac{0.706}{T_i^{\text{iso}}(\omega, \tau_\alpha)} + \frac{0.289}{T_i^{\text{iso}}(\omega, \tau_\beta)}. \quad (15'')$$

This leads to a different solution for the two correlation times τ_L and τ_S . In particular, the longer correlation time is drastically increased as compared to case (a) due to the suppression of the coefficient of the first term in Eq. (15''). The result of this calculation is reported in Fig. 5(b). From Eq. (15'') the estimated value of the longitudinal relaxation time at 400 MHz is $T_1=480$ ms, less than the actual measurement, but not exceedingly so. Therefore, from our relaxation investigation, we cannot uniquely assert which of the two geometries describes the adsorption of water molecules on the glass surface. However, the similar trend of both Figs. 5(a) and 5(b) indicates that the dynamics of the molecules is slower as the sample undergoes the drying process.

The range of the submonolayer interval investigated was constrained by poor signal-to-noise ratio considerations which prevented us from performing precise quantitative experiments at very low coverage conditions, and by the fact that the water content may vary slightly during the sealing procedures. However, we observed a small proton NMR signal at 27 MHz on the sample sealed in a test tube after evacuation at 150°C. The transverse relaxation time was of the order of 0.4 ms, i.e., comparable to the values at the lowest coverage reported. On the other hand, the longitudinal relaxation time appeared to be extremely long, perhaps as much as of the order of 1 s. The observed signal may originate from OH silanol groups chemically bound to the surface. In that case, the transverse relaxation time would be given by the rigid lattice limit where the value of r in Eqs. (17)–(19) would be the distance between OH groups. Taking a surface concentration of OH groups for silica to be the typical value of 4.6 nm^{-2} ,²³ and assuming a hexagonal lattice structure, the transverse relaxation time would be about 30 times smaller than the one observed and would not be detected in our spin-echo experiments. It is more likely that the observed signal comes from a small amount of surface water.

The evolution of the correlation times below one monolayer may be compared with the results of PFG measurements. In this range of coverage the values of the measured self-diffusion coefficient are smaller than

that predicted by the linear dependence on water content suggested by Archie's law. This can only be attributed to a decrease in translational motion, typical of surface diffusion. This is consistent with the observed increase of the correlation times characteristic of the relaxation processes described above, suggesting that there may be some connection between rotational and translational degrees of freedom. For example, it may be assumed that reorientation around an axis perpendicular to the surface happens every time a molecule jumps from one surface site to the next. In that case the diffusion coefficient is estimated to be

$$D = l^2/6\tau_S, \quad (22)$$

where l is the jump distance. If we consider that the surface associated with one water molecule is 10.6 \AA^2 and that water is arranged, for simplicity, in a hexagonal structure, we obtain $l=3.5 \text{ \AA}$. In Fig. 6 the self-diffusion coefficient estimated from the short correlation time τ_S is compared with the values measured from NMR PFG experiments as a function of water content below one monolayer. The estimate from both the molecular orientations is displayed in Fig. 6, suggesting that case (b) may be more representative. Although there is qualitative correspondence between measured diffusivity and values from relaxation measurements, it has to be emphasized that the experimental self-diffusion coefficient is a macroscopic quantity appropriate to a region much larger than that characteristic of the porous structure. Therefore, it is expected to be an underestimate of the value relative to short-length scales, which is the one connected to a jump probability. This simply suggests that the jump rate is less effective in reorienting the water molecules or that there is finite probability for jumps to sites more than one molecular distance apart.

It is interesting to compare the diffusion experiments on this sample with those reported earlier on sol-gel silica glasses.^{4,7} In that case a strong contribution to the overall

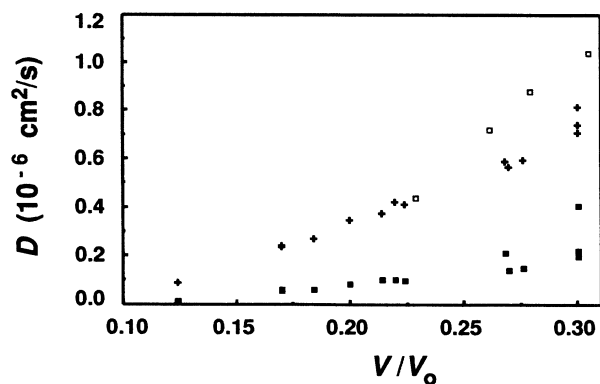


FIG. 6. Experimental submonolayer diffusion coefficient (\square) is compared with the estimates (\blacksquare), ($+$) given by Eq. (22), using two possible models for the short correlation time τ_S corresponding to Figs. 5(a) and 5(b). There appears to be qualitative agreement between measured and estimated diffusion coefficients for the latter case where one O—H bond is parallel to the surface.

self-diffusion constant was observed due to the vapor phase permeating the liquid-solid system under unsaturated conditions. Such a contribution is not found in the present case. It seems reasonable to attribute this to the different characteristic geometry of the different media. In fact, the sol-gel glass samples had a larger porosity ($\phi=0.85$) and, more importantly, larger pore size ($d=95$ and 240 nm). The smaller pore size of the sample in the present experiment leads to a suppression of vapor-phase diffusion owing to a shorter mean free path. This effect is described by the Knudsen term in Eq. (3) of Ref. 4.

VI. CONCLUSIONS

The combination of NMR relaxation (longitudinal and transverse) and self-diffusion measurements of water in porous media helps in understanding the dynamics of fluids in random geometries.

When the amount of liquid present in the porous space exceeds that corresponding to the first adsorbed monolayer, the experiments prove that the fluid-solid system in the present study is homogeneous, at least over length scales larger than a few micrometers. The linear dependence between the relaxation times and the fraction of pore space occupied by the liquid also indicates that the interaction responsible for the relaxation is confined to the first monolayer. The coverage dependence of the self-diffusion coefficient indicates that the only obstacle to macroscopic transport is due to the geometrical tortuosity of the diffusion path and can be described by the phenomenological Archie's law.

The difference in the absolute values of the longitudinal and transverse relaxation times, and their small frequency dependence in the range 11–400 MHz, require that at

least two elementary processes describe the microscopic dynamics of the water molecules interacting with the surface.

When the amount of liquid present in the porous space is less than that corresponding to the first adsorbed monolayer, the relaxation rates are observed to increase above the values predicted by assuming no evolution of the molecular interaction during drying. Considering a model with two rotational degrees of freedom for the water molecules, the longitudinal and transverse relaxation times provide values for the two correlation times at each submonolayer coverage, both of which increase upon drying. This observation is consistent with the hypothesis that molecules become more bound to the surface when the water content is decreased below one monolayer. This is also revealed from the behavior of the self-diffusion coefficient in the same interval of coverage. Comparison between the two results leads us to conclude that rotational and translational degrees of freedom are strongly interrelated, suggesting that an adsorbed water molecule is allowed to rotate only during a jump to a near-neighbor site and that, most likely, one of the O—H bonds rotates in the plane of the surface.

ACKNOWLEDGMENTS

This work was supported by the Department of Energy, Grant No. DE-FG02-86ER45251 (F.D.'O. and W.P.H.) and the National Science Foundation, Science and Technology Center for Advanced Cement Based Materials under Grant No. DMR-8808432 (S.B. and W.P.H.). The gas-sorption equipment was obtained thanks to the Department of Energy, Grant No. DE-FG05-86ER75295.

¹See, for example, *Molecular Dynamics in Restricted Geometries*, edited by J. Klafter and J. M. Drake (Wiley, New York, 1989).
²F. D'Orazio, J. C. Tarczon, W. P. Halperin, K. Eguchi, and T. Mizusaki, *J. Appl. Phys.* **65**, 742 (1989).
³W. P. Halperin, F. D'Orazio, S. Bhattacharja, and J. C. Tarczon, in *Molecular Dynamics in Restricted Geometries* (Ref. 1), pp. 311–350.
⁴F. D'Orazio, S. Bhattacharja, W. P. Halperin, and R. Gerhardt, *Phys. Rev. Lett.* **63**, 43 (1989).
⁵J. R. Banavar and L. M. Schwartz, *Phys. Rev. Lett.* **58**, 1411 (1987); in *Molecular Dynamics in Restricted Geometries* (Ref. 1), pp. 273–309.
⁶S. Bhattacharja, F. D'Orazio, J. C. Tarczon, W. P. Halperin, and R. Gerhardt, *J. Am. Ceram. Soc.* **72**, 2126 (1989).
⁷F. D'Orazio, S. Bhattacharja, W. P. Halperin, and R. Gerhardt, *Phys. Rev. B* **42**, 6503 (1990).
⁸D. P. Gallegos, D. M. Smith, and C. J. Brinker, *J. Colloid. Interface Sci.* **124**, 186 (1988).
⁹G. E. Archie, *Trans. AIME* **146**, 54 (1942).
¹⁰H. Tanaka, T. Yazawa, K. Eguchi, H. Nagasawa, N. Matsuda, and T. Einishi, *J. Non-Cryst. Solids* **65**, 301 (1984).

¹¹S. Meiboom and D. Gill, *Rev. Sci. Instrum.* **29**, 688 (1958).
¹²J. E. Tanner, *J. Chem. Phys.* **52**, 2523 (1970).
¹³K. Fukuda, T. Kasuga, T. Mizusaki, A. Hirai, and K. Eguchi, *J. Phys. Soc. Jpn.* **58**, 1662 (1989).
¹⁴M. R. Rao and J. M. Smith, *AIChE J.* **10**, 293 (1964).
¹⁵J. M. Smith, *Chemical Engineering Kinetics* (McGraw-Hill, New York, 1970), p. 418.
¹⁶M. Sahimi and V. L. Jue, *Phys. Rev. Lett.* **62**, 629 (1989).
¹⁷N. Bloembergen, E. Purcell, and R. Pound, *Phys. Rev.* **73**, 679 (1948).
¹⁸D. E. Woessner and J. R. Zimmerman, *J. Phys. Chem.* **67**, 1590 (1963).
¹⁹A. Odajima, J. Sohma, and S. Watanabe, *J. Chem. Phys.* **31**, 276 (1959).
²⁰D. E. Woessner, *J. Chem. Phys.* **36**, 1 (1962).
²¹H. Pfeiffer, in *NMR Basic Principles and Progress*, edited by P. Diehl, E. Fluck, and R. Kosfeld (Springer-Verlag, New York, 1972), Vol. 7, pp. 53–153.
²²R. Kubo and K. Tomita, *J. Phys. Soc. Jpn.* **9**, 888 (1954).
²³J. A. G. Taylor, J. Hockey, and B. A. Pethica, *Proc. Br. Ceram. Soc.* **5**, 133 (1965).